

ACTIVATED CLIQUES: NETWORK-BASED ACTIVATION DETECTION IN TASK-BASED FMRI

Shu Zhang^{1,2}, Jinglei Lv^{1,2}, Xiang Li¹, Xi Jiang¹, Lei Guo², Tianming Liu¹

¹Cortical Architecture Imaging and Discovery Lab, Department of Computer Science, The University of Georgia, Athens, GA; ²School of Automation, Northwestern Polytechnical University, Xian, China

ABSTRACT

Human brain function has been widely believed as a network behavior. However, most previous activation detection methods in the task-based fMRI field were voxel-based, instead of network-based. For instance, the general linear model (GLM) has been widely used to fit the external stimulus curve with the fMRI BOLD signal of each voxel. In this paper, we present a novel network-based activation detection method to fit network-level measurement of the brain's response with the external stimulus curve. The basic idea here is that based on the structural connectome constructed from DTI data, the propensity for synchronization (PFS) of combinations of three-nodes complete graphs, or cliques, is calculated from task-based fMRI signals, and the general linear model is then used to detect activations of the network-centric PFS curve. Further, given the intrinsically-established correspondences of structural connectomes and the derived complete graph cliques, the individual activation detection results are assessed across a population using the existing FSL FLAME framework to determine group-wise activated cliques during task performance. Our experimental results demonstrated that the network-based activation detection method is complementary to the widely-used voxel-based activation detection methods.

Index terms— Activation detection, DICCCOL, task-based fMRI, general linear model.

1. INTRODUCTION

Voxel-based activation detection in task-based fMRI has been widely used in the human brain mapping field. For instance, the general linear model (GLM) [13, 14] has been commonly used to determine activated voxels in task-based fMRI images. However, the voxel-based activation detection method has limitations in terms of elucidating the complex functional brain activities, since it has been generally believed that brain function is a network behavior. In response to this limitation, recently, we developed and applied a fiber-centered activation detection method in [1] to reveal the activated connectivity patterns and our results have suggested that activated fiber-connected regions cover substantially wider cortical areas than the traditional voxel-based activation methods. More recently, we examined the temporal dynamics of functional connectivity during task performance [2] and our extensive experimental results [2] showed that the whole-brain's functional connectivity pattern well correlated with the block-based external stimulus curve. These results in [1, 2] demonstrated the feasibility and promise of connectivity-based activation detection in task-based fMRI.

Inspired by the above promising direction [1, 2], in this paper, we designed and applied a novel *network-based* activation detection framework that aims to determine the activated complete graphs with three nodes, or cliques, based on structural connectomes derived from DTI (diffusion tensor imaging) data. The basic premise is that the temporally varying functional synchronization among these graph cliques would be similar to the external block-based stimulus curve, assuming that the participating human subject is following the instruction of task-based paradigm [1, 2]. Then, the activation level of the network or the graph clique is determined by the commonly-used GLM that is applied on the functional synchronization curve. Since it is not known in advance which complete three-nodes graph cliques would be involved in the task-performance, we perform a data-driven whole-space search within all possible combinations of nodes that are more likely to be involved in the task performance within a structural connectome, which is constructed based on our recently developed and validated DICCCOL (Dense Individualized and Common Connectivity-based Cortical Landmarks) system [3] (<http://dicccol.cs.uga.edu/>). A prominent attribute of the DICCCOL system (358 landmarks) is that each cortical landmark has intrinsically-established correspondence across individual brains, and thus the structural connectomes and derived three-nodes complete graph cliques based on DICCCOL also have correspondences across individual brains. In this way, the activation level measured by the GLM for each complete graph clique can be assessed at the population level by pooling the activation detection results from multiple brains. Essentially, this group-wise network-based activation detection methodology is deemed to have more robustness to noises and variabilities, since a variety of prior studies have already demonstrated the advantages of group-wise activation detection [15, 16]. We have applied the proposed novel methods on a working memory task-based fMRI dataset [6] and our experimental results demonstrated that the network-based activation detection method is complementary to the voxel-based activation detection methods.

2. MATERIALS AND METHODS

2.1. Overview

The computational pipeline of our methods is summarized in Fig. 1. In the methods, we first used DTI data to identify the structural connectomes in each brain via the DICCCOL system in [3]. Then, as shown in Fig.1a, a landmark-based activation detection methodology is applied to detect activated landmarks for the purpose of significantly narrowing down the prohibitively huge search space (the total number is C_{358}^3) of possible three-nodes cliques among the DICCCOL-based structural connectome. Our rationale here is that the activated landmarks determined via the

first round of landmark-based activation detection are more likely to be involved in the activated networks. In this step in Fig.1a, we perform the activation detection on the single landmark through the general linear model (GLM) [1, 2]. Then, the significance of activation level of each landmark is assessed at the population level given the correspondences of the 358 DICCCOL landmarks across individuals [3]. In this way, we identified 45 consistently activated DICCCOL landmarks to be the ROI (regions of interest) set for the second stage of network-based activation detection, as shown in Fig.1b. Specifically, the functional synchronization curves measured by the propensity for synchronization (PFS) [10, 11] are derived within all possible combinations of three-nodes graph cliques, which are determined from the first stage of landmark-based activation detection (45 DICCCOLs). Then, the propensity for synchronization (PFS) is measured based on fMRI time series within each graph clique, and the GLM model is applied on the PFS curve, instead of raw fMRI BOLD signal, to assess the similarity between external stimulus curve and the PFS curve. Finally, the significance of activation level of each corresponding clique is assessed in a group of 20 subjects, which is enabled by the intrinsically-established correspondences of the DICCCOL-based structural connectomes. Given the activation detection results by both methodologies, we compared their activation patterns and concluded that their results are complementary.

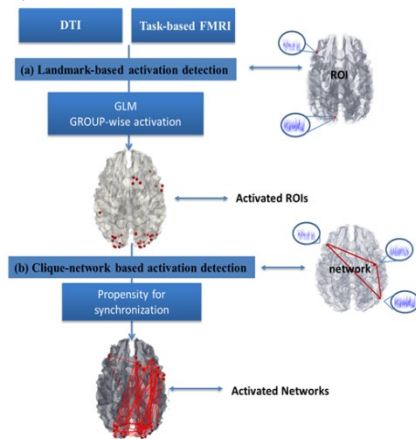


Fig.1. The overview of our method is shown in Fig 1, (a) landmark-based method (b) DICCCOL-triple network based activation detection (c) Display the method that compare the result from two methods and get the conclusion from the result.

2.2. Data acquisition and pre-processing

In an operational span (OSpan) working memory task-based fMRI experiment under IRB approval [6], 20 healthy young adult subjects were scanned and fMRI images were acquired on a 3T GE Sigma scanner at the Bioimaging Research Center of The University of Georgia. Briefly, acquisition parameters are as follows: fMRI: 64×64 matrix, 4mm slice thickness, 220mm FOV, 30 slices, TR=1.5s, TE=25ms, ASSET=2. Each participant performed a modified version of the OSpan task (3 block types: OSpan, Arithmetic, and Baseline) while fMRI data was acquired [6]. DTI data was acquired with dimensionality 128×128×60, spatial resolution 2mm×2mm×2mm; parameters were TR 15.5s and TE 89.5ms, with 30 DWI gradient directions and 3 B0 volumes acquired. The fMRI data was co-registered with the DTI image space using a linear transformation via FSL FLIRT. For more details about pre-processing, please refer to [3, 5, 7].

2.3. Structural connectomes and landmark-based activation detection method

Recently, we identified a dense map of 358 consistent cortical landmarks, or regions of interest (ROIs), in over 240 brains, named Dense Individualized and Common Connectivity-based Cortical Landmarks (DICCCOL) [3]. The visualizations, models, and prediction source codes of these 358 DICCCOLs have been released online at: <http://dicccol.cs.uga.edu/>. A prominent feature of these 358 DICCCOLs is that they possess intrinsically established structural and functional correspondences across individuals and populations [3]. Therefore, these DICCCOLs offer a natural substrate for fMRI activation detection without the need of image registration and spatial smoothing, which are commonly used in traditional fMRI signal analysis methods. Essentially, due to the lack of a quantitative representation of common brain architecture, most previous fMRI activation detection methods rely on spatial normalization and spatial smoothing to deal with the anatomical variation of different brains [1, 2]. However, a variety of recent studies have demonstrated that spatial normalization and smoothing could significantly reduce the sensitivity and specificity of task-based fMRI activation detection [8, 9].

Therefore, in this paper, we first implemented a landmark-based activation detection framework based on DICCCOLs to explore the activation significance of each individual landmark among a group of brains, as illustrated in Fig.1a. Our rationale here is the same as that in other group-wise fMRI activation detection methods [15, 16]. That is, group-wise approach improves the statistical power and reliability of individual fMRI studies. Specifically, for each landmark, we first set the estimated activation significance parameters and their estimation deviations from a group of subjects, which were generated from the application of GLM on fMRI signals of each DICCCOL ROI in individual brains. These significance levels are used as the input of group-wise t-statistics via the tool of FSL FLAME as the second level of group analysis [15]. Then, the derived p-value from the group-level t-statistics is further translated to the commonly-used z-score to measure the group-wise activation significance of each DICCCOL landmark. Afterwards, we determined the activated DICCCOL landmarks via a widely-used threshold method. From the group-wise activation detection, we already obtained 45 consistently activated ROIs (z-score threshold at 2.0) among the 358 DICCCOLs to construct a working memory network, which will be further used to test our network-based activation detection method. It should be noted that these 45 consistently activated DICCCOL ROIs already covered much more cortical regions than the results in [4, 7] via the traditional voxel-based fMRI activation detection, suggesting the superiority of the DICCCOL-based group-wise landmark activation detection method.

2.4. Network-based activation detection methods

Although the 45 consistently activated DICCCOL ROIs are deemed to be more likely involved in working memory network, we do not know which sub-networks, or graph cliques, among these 45 ROIs are specifically activated during the working memory task performance. In response to this challenge, we employ a data-driven approach and search all possible combinations of three-nodes cliques within the working memory network. In this paper, each three-nodes sub-network, or graph clique, is considered as a potential sub-network, in which the functional synchronization and activation significance are assessed in the following sections.

3. RESULT

2.4.1 Calculate the PFS for the sub-network

The PFS is a graph theoretic parameter that can be used to represent the functional synchronization behavior in a networked system [10, 11]. Thus, we first describe a functional brain network by a weighted undirected graph $G=(V, E)$, where each node $v_i \in V$ is an DICCCOL ROI involved in the working memory system, and while edges E denotes the connectivity between ROIs regarding to the fMRI BOLD signal similarity. The Laplacian matrix of graph G [10, 11] is derived as follows:

$$L(i, j) = \begin{cases} 1 & \text{if } i = j \\ -\frac{w(i, j)}{\sqrt{d_i d_j}} & \text{otherwise} \end{cases} \quad (1)$$

where $d_i = \sum_j w(i, j)$ is defined as the degree of the node $v_i \in V$. The set of eigenvalues of L , $0 = \lambda_1 \leq \lambda_2 \leq \dots \leq \lambda_N$, are defined as spectrum of L and PFS are defined as the eigen ratio $r = \lambda_N / \lambda_2$, which was used as an indicator to characterize the network synchronization [10, 11]. A smaller value of PFS indicates that synchronization of brain networks tends to be more stable, and vice versa. Please refer to [10, 11] for more details of PFS.

2.4.2 Clique activation detection based on PFS

Now we are able to measure the network-level response within the cliques to external stimulus via the GLM method [13, 14]. For each of a group of 20 subjects, we tested every possible combination of 3 landmarks among the 45 working memory ones as a triple clique network, and the total number of combinations is 14190, as visualized in Fig. 2a. After applying the GLM method on the PFS curve for the comparison with the external block-based stimulus curve, as illustrated in Figs. 2b and 2c, we can obtain the similar significance level of each PFS curve. Afterwards, we employed the widely-used FSL FEAT [12] for this procedure, and each of the 14190 cliques (arranged in Fig. 2) was analyzed in a similar way.

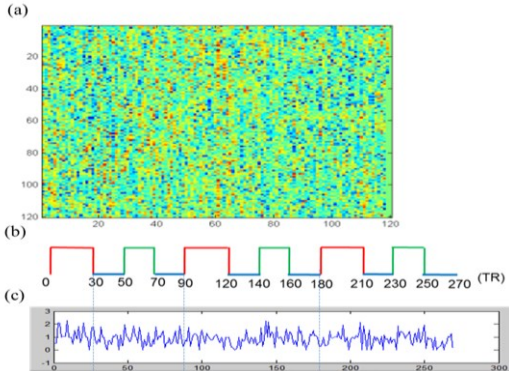


Fig.2. (a) 14190 points are arranged in the picture, in which each pixel means a PFS value for a clique network. (b) Task-based stimulus curve. (c) An example of activation network's PFS time series.

In the last step, the derived p-value from the group-wise t-statistics is further translated to the commonly used z-score to measure the activation significance of each network's PFS curve. We determined the activated networks via a widely-used thresholding method and the threshold was chosen empirically.

3.1 Activation detection result

The results of landmark-based activation detection are shown in Fig. 3a. The corresponding results for the network-based activation detection using different z-score thresholds are shown in Figs.3b-3d. It can be clearly seen that the activated network cliques are quite dense among the corresponding landmarks, e.g., 249 activated networks among the 45 activated ROIs when the z-score threshold was set as 12. This result not only provides support to our previous premise that activated landmarks are more likely to be involved in activated networks, but also suggests that network-level activities are highly synchronous with the external stimulus curve. This result further confirms our prior studies in [1, 2] and importantly, offers novel insights on the network-level functional behaviors of the brain during task performance.

It is also evident that with the increase of z-score threshold, the numbers of activated networks become less and less. However, it is interesting that the distributions of the most consistently activated networks are similar across different thresholds, suggesting the robustness of network-based activation detection. This result indicates that network-based activation detection method can provide useful perspectives to the functional activities of the brain during task performance. Here, the visualizations in Figs. 3b-3d clearly demonstrates the strong functional interactions among the clique networks in the occipital and frontal lobes, which is consistent with current neuroscience knowledge [4]. For comparison purpose, both of the activated and deactivated cliques (detected by the inverse of stimulus curve in Fig. 2b) in the working memory network are shown in Fig. 4. It is interesting that the numbers of both activated and deactivated networks are comparable, suggesting the complexity of functional brain network behaviors in task performance. The neuroscience interpretation of the results in Fig. 4 warrants extensive investigation in the future.

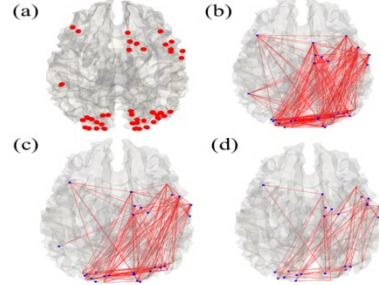


Fig.3. (a) 45 ROIs are shown in part(a). (b) When $Z=12$, the number of networks is 249. (c) When $Z=14$, the number of networks is 91. (d) When $Z=16$, the number of networks is 30.

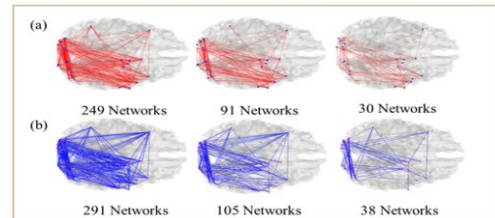


Fig.4. Distribution of activated and deactivated cliques on the cortical surface, (a) Activated cliques. (b) Deactivated cliques. Z-scores correspond to those in Figs.3b-3d from the left to right.

3.2 Comparison of results by two methods

For each activated working memory ROI, we quantitatively compared the number of activated networks that each ROI is involved in (Fig. 5a) and the activation level z-score determined in landmark-based activation detection (Fig. 5b). It is interesting that some working memory ROIs, such as DICCCOL #11, #17, #24, #235 and #248 (Fig. 5a), are strongly activated in both landmark-based activation detection and network-based activation detection. While other working memory ROIs, such as DICCCOL #280 and #282, are much more strongly activated in network-based activation detection than landmark-based activation detection, suggesting that landmarks that are very active in network behaviors are not necessarily very much following the external stimulus curve, as measured by the GLM on raw fMRI BOLD signals. This result indicates that network-based activation detection is complementary to landmark-based or voxel-based activation detection methods, and can offer novel insights in the functional activities of the brain during task performance. In Fig. 5, we can also see some working memory ROIs, such as DICCCOL #1, #2, #4, and #16, that are strongly active in landmark-based activation detection but not necessarily strongly active in network-based activation detection. This result further demonstrates the complementary nature of these two activation detection methods.

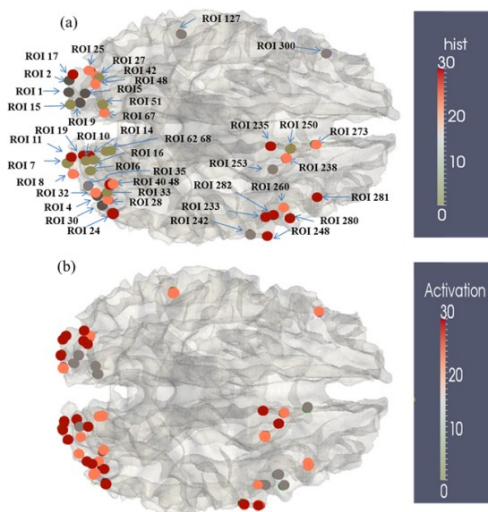


Fig.5. (a) The numbers of activated networks that each DICCCOL ROI was involved in. It is color-coded based on the bar on the right. (b) The z-scores obtained from group-wise landmark-based activation detection for 45 DICCCOL ROIs. They are color-coded according to the bar on the right. Additional visualizations of the DICCCOLs are available at: <http://dicccol.cs.uga.edu/>

4. CONCLUSION

We presented a novel network-based fMRI activation detection framework that is implemented in two stages. The first stage performed a landmark-based activation detection to identify those most consistently activated ROIs. The second stage performed a network-based activation detection method that relied on comparing the functional synchronization curves of networks with the external stimulus curve via the GLM. In both stages, the activation detections were conducted at the group level given the intrinsic correspondences provided the structural connectome. The application of this novel framework on a working memory task-based fMRI dataset demonstrated that the network-based activation

detection method is complementary to the landmark-based activation detection methods, and offered novel insights into the functional interactions at the network level in the brain during task performance. In the future, we plan to investigate effective and efficient approaches to deriving other types of graphs or cliques among the DICCCOL-based connectomes and examine their activation patterns in fMRI.

REFERENCE

- [1] Lv J, Guo L, Li K, Hu X, Zhu D, Han J, Liu T, Activated Fibers: Fiber-centered Activation Detection in Task-based FMRI, IPMI, 2011.
- [2] Li X, Lim C, Li K, Guo L, Liu T, Detecting Brain State Changes via Fiber-Centered Functional Connectivity Analysis, Neuroinformatics, in press, 2012.
- [3] Zhu, D., Li, K., Guo, L., Jiang, et al., DICCCOL: Dense Individualized and Common Connectivity-Based Cortical Landmarks. Cerebral Cortex, in press, (2012).
- [4] Faraco CC, Unsworth N, Langley J, Terry D, Li K, Zhang D, Liu T, Miller LS, Complex span tasks and hippocampal recruitment during working memory, NeuroImage 55(2): 773-787, 2011.
- [5] Li K., et al., Individualized ROI Optimization via Maximization of Group-wise Consistency of Structural and Functional Profiles. In: Neural Information Processing Systems (NIPS), 2010.
- [6] Faraco CC, Unsworth N, Langley J, Terry D, Li K, Zhang D, Liu T, Miller LS, Complex span tasks and hippocampal recruitment during working memory, NeuroImage 55(2): 773-787, 2011.
- [7] Zhu D., Li K., Faraco C.C., Deng F., Zhang D., Guo L., et al., Optimization of functional brain ROIs via maximization of consistency of structural connectivity profiles, NeuroImage 59(2):1382-93, 2011.
- [8] Bertrand T, et al., Analysis of a large fMRI cohort: Statistical and methodological issues for group analyses. NeuroImage 35 105–120. (2007).
- [9] Li Y, et al., TwinMARM: two-stage multiscale adaptive regression methods for twin neuroimaging data. IEEE Trans Med Imaging; 31(5):1100-12. 2012.
- [10] Hu X, Guo L, Zhu D, Li K, Zhang T, Lv J, Han J, Liu T, Assessing the dynamics on functional brain networks using spectral graphy theory, IEEE International Symposium on Biomedical Imaging, 2011.
- [11] Chung, F., Spectral graph theory, 1997: American Mathematical Society.
- [12] Smith, S. M., M. Jenkinson, et al., Advances in functional and structural MR image analysis and implementation as FSL. Neuroimage 23: S208-S219(2004).
- [13] Friston, K.J., et al., Statistical parametric maps in functional imaging: a general linear approach. Human brain mapping, 1994. 2(4): p. 189--210(1994).
- [14] Worsley, K. J. An overview and some new developments in the statistical analysis of PET and fMRI data. Hum Brain Mapp 5(4): 254-258(1997).
- [15] Beckmann C.F., Jenkinson M., and Smith S.M.. General multi-level linear modelling for group analysis in FMRI. NeuroImage, 20:1052-1063 (2003).
- [16] Thirion B., et al., Analysis of a large fMRI cohort: Statistical and methodological issues for group analyses. NeuroImage 35 105–120. (2007).